Viscosity and Diffusion Constants Calculation of *n*-Alkanes by Molecular Dynamics Simulations

Song Hi Lee* and Taihyun Chang†

Department of Chemistry, Kyungsung University, Busan 608-736, Korea
†Department of Chemistry and Center for Integrated Molecular System, Pohang University of Science and Technology, Pohang 790-784, Korea
Received July 23, 2003

In this paper we have presented the results for viscosity and self-diffusion constants of model systems for four liquid *n*-alkanes (C_{12}, C_{20}, C_{32}, and C_{44}) in a canonical ensemble at several temperatures using molecular dynamics (MD) simulations. The small chains of these *n*-alkanes are clearly $<R_{ee}^2>/6<R_g^2>>1$, which leads to the conclusion that the liquid *n*-alkanes over the whole temperatures considered are far away from the Rouse regime. Calculated viscosity η and self-diffusion constants D are comparable with experimental results and the temperature dependence of both η and D is suitably described by the Arrhenius plot. The behavior of both activation energies, E_η and E_D, with increasing chain length indicates that the activation energies approach asymptotic values as n increases to the higher value, which is experimentally observed. Two calculated monomeric friction constants ζ and ζ_D give a correct qualitative trend: decrease with increasing temperature and increase with increasing chain length n. Comparison of the time auto-correlation functions of the end-to-end vector calculated from the Rouse model for *n*-dodecane (C_{12}) at 273 K and for *n*-tetratetracontane (C_{44}) at 473 K with those extracted directly from our MD simulations confirms that the short chain *n*-alkanes considered in this study are far away from the Rouse regime.

Key Words : MD simulation, Viscosity, Diffusion, *n*-Alkanes

Introduction

Experimental measures on the viscosity (η) and the self-diffusion constant (D) of polymer melts have often been used to test molecular theories of transport properties.[1,2] The polymer chain dynamics of unentangled and entangled chains are commonly described by the Rouse model and the reptation model, respectively, which predict:[1,3,4]

$$\begin{aligned} D &\sim M^{-1} \text{ and } \eta \sim M^{1} \quad \text{for} \quad M < M_e, \\ D &\sim M^{-2} \text{ and } \eta \sim M^{3.4} \quad \text{for} \quad M > M_e. \end{aligned} \tag{1}$$

where M_e is the entanglement coupling molecular weight. At the molecular weight below the Rouse regime, D and η of *n*-alkanes show power law behaviors. For example, D of *n*-alkanes from *n*-octane to polyethylene of the molecular weight of several thousands was reported to follow the relation, $D \sim M^{-\alpha}$ in which the exponents a is in the range of 2.72-1.85 depending on temperature.[5-7] Although the power law dependence has the same functional form as in Eq. (1), the origin is totally different. The molecular weight dependence of D and η in Eq. (1) is attributed to the topological entanglement effect not the segmental friction while the exponent found below the Rouse regime reflects the molecular weight dependence of the local friction not the topological effect. A property often employed to investigate the local friction in the polymer chain dynamics is the monomeric friction constant, ζ. For low molecular weight polymers, ζ depends on the molecular weight. Above the onset molecular weight at which the Rouse behavior is observed, ζ becomes independent of molecular weight.[3,8] Recent molecular dynamics (MD) simulation studies showed that the Rouse chain behavior of *n*-alkane was obtained around 80 carbons at which ζ reaches an asymptotic limit independent of molecular weight.[9,10]

In a recent study,[11] diffusion of methyl yellow (MY) in the oligomeric host of *n*-alkanes and *n*-alcohols was studied by forced Rayleigh scattering as a function of the molecular weight and the viscosity of the medium. It was observed that the diffusivity of the probe molecule follows a power law dependence on the molecular weight of the oligomers, $D_{MY} \sim M^{-\alpha}$ well. As the molecular weight of the oligomers increases, the exponent shows a sharp transition from 1.88 to 0.91 near docosane (C_{22}) in *n*-alkanes and from 1.31 to 0.60 near 1-hexadecanol ($C_{16}OH$) in *n*-alcohols at 45 °C. A similar transition was also found in the molecular dynamics (MD) simulation for the diffusion of a Lennard-Jones particle of a size similar to MY in *n*-alkanes. This transition deems to reflect a change of the dynamics of oligomeric chain molecules that the motion of the segments, not the entire molecules, becomes responsible for the transport of the probe molecule as the molecular weight of the oligomer increases.

While the Rouse-reptation crossover has received considerable attention in recent years,[2-8] the *n*-alkane-Rouse crossover has received relatively little attention. The equilibrium (EMD) and non-equilibrium molecular dynamics (NEMD) simulations[12-14] on the system are useful methods for the study on the transport properties of liquid *n*-alkanes of

*Corresponding author. e-mail: shlee@star.ks.ac.kr

moderate molecular sizes (C_{10}-C_{40}), which can shed light on the polymer dynamics in the molecular level.

In this study, we adopt the Green-Kubo and Einstein formulas for the calculation of the viscosities and diffusion constants of liquid *n*-dodecane ($C_{12}H_{26}$), *n*-eicosane ($C_{20}H_{42}$), *n*-dotriacontane ($C_{32}H_{66}$), and *n*-tetratetracontane ($C_{44}H_{90}$) using EMD simulation. The primary purpose of this study is to characterize the viscosity and self-diffusion dynamics of small *n*-alkanes as a function of chain length n (or molecular weight M) and as a function of temperature. In general the temperature dependence of the diffusion constant of small *n*-alkanes is well described by the Arrhenius equation, $D \sim \exp(-E_D/RT)$, while the temperature dependence of the viscosity of polyethylene is often assumed to follow the Arrhenius law, but the experimental result for the linear polyethylene shows that the temperature dependence, as in most polymers, does not obey the Arrhenius law.[6] In the following section, we describe the technical details of MD simulation. We present some theoretical aspects in section III, our results in section IV, and the concluding remarks in section V.

Molecular Models and MD Simulation Methods

For liquid *n*-alkanes, we have chosen 4 systems - *n*-dodecane ($C_{12}H_{26}$), *n*-eicosane ($C_{20}H_{42}$), *n*-dotriacontane ($C_{32}H_{66}$), and *n*-tetratetracontane ($C_{44}H_{90}$). Each simulation was carried out in the NVT ensemble; the number of *n*-alkane molecules was N=100, the density and hence the length of cubic simulation box were fixed and listed in Table 1 for given temperatures. The usual periodic boundary condition in the x-, y-, and z-directions and the minimum image convention for pair potential were applied. Constraint method was used to keep the temperature of the system constant.[15,16]

We used a united atom (UA) model for *n*-alkanes, that is, methyl and methylene groups are considered as a spherical interaction site centered at each carbon atom. The interaction between the sites on different *n*-alkane molecules and between the sites separated by more than three bonds in the same *n*-alkane molecule was described by a Lennard-Jones (LJ) potential. All the sites in a chain have the same LJ size parameter $\sigma_i = \sigma_{ij} = 3.93$ A, and the well depth parameters were $\varepsilon_i = 0.94977$ kJ/mol for interactions between the end sites and $\varepsilon_i = 0.38911$ kJ/mol for interactions between the internal sites. The Lorentz-Berthelot combining rules [$\varepsilon_{ij} = (\varepsilon_i\varepsilon_j)^{1/2}$, $\sigma_{ij} = (\sigma_i + \sigma_j)/2$] were used for interactions between an end site and an internal site. A cut-off distance of 2.5 σ_i was used for all the LJ interactions.

The bond-stretching was ignored by a constraint force which keeps intramolecular nearest neighbors at a fixed distance using RATTLE algorithm.[17] The bond bending interaction was also described by a harmonic potential with an equilibrium angle of 114° and a force constant of 0.079135 kJ/mol/degree^2. The torsional interaction was described by the potential developed by Jorgensen *et al.*[18]:

$$U_{torsion}(\phi) = a_0 + a_1\cos\phi + a_2\cos^2\phi + a_3\cos^3\phi, \quad (2)$$

where ϕ is the dihedral angle, and $a_0 = 8.3973$ kJ/mol, $a_1 = 16.7862$ kJ/mol, $a_2 = 1.1339$ kJ/mol, and $a_3 = -26.3174$ kJ/mol.

For the time integration of the equations of motion, we adopted velocity Verlet algorithm[19] with a time step of 5 femto-second for all the systems. After a total of 10,000,000-20,000,000 time steps (50-100 nano-seconds) for equilibration, the equilibrium properties were then averaged over 5 blocks of 2,000,000 time steps(50 nano-seconds). The configurations of all the molecules for further analyses were stored every 10 time steps (0.05 pico second) which is small enough for the tick of any time auto-correlation functions.

Two routes for self-diffusion constant from EMD simulations: the Green-Kubo relation from the velocity autocorrelation (VAC) function and the Einstein relation from the mean square displacement (MSD) are[20]

$$D = \frac{1}{3}\int_0^\infty dt \langle \mathbf{v}_i(0)\cdot\mathbf{v}_i(t)\rangle . \quad (3)$$

and

$$D = \frac{1}{6}\lim_{t\to\infty}\frac{d}{dt}\langle[\mathbf{r}_i(t)-\mathbf{r}_i(0)]^2\rangle . \quad (4)$$

Table 1. MD simulation parameters for molecular models of *n*-alkanes

n-alkanes	T (K)	Density (g/mL)[a]	Length of box (A)	*n*-alkanes	T (K)	Density (g/mL)[a]	Length of box (A)
n-$C_{12}H_{26}$	273	0.7636	33.335	n-$C_{20}H_{42}$	273	0.8021	38.819
(14.195)[b]	293	0.7487	33.555	(14.128)[b]	293	0.7888	39.036
	311	0.7360	33.747		311	0.7769	39.234
	333	0.7194	34.004		333	0.7621	39.486
	372	0.6907	34.469		372	0.7361	39.946
n-$C_{32}H_{66}$	311	0.8007	45.388	n-$C_{44}H_{90}$	311	0.8135	50.185
(14.090)[b]	333	0.7869	45.653	(14.073)[b]	333	0.7993	50.480
	372	0.7626	46.132		372	0.7745	51.014
	423	0.7307	46.795		423	0.7418	51.752
	473	0.6995	47.481		473	0.7099	52.517

[a]Densities of *n*-alkanes are obtained from or interpolated (or extrapolated) from the values at liquid states in Ref. 29. [b]Mass of monomer (g/mole).

The corresponding Green-Kubo and the Einstein relations for the viscosity are very similar to those for D:

$$\eta = \frac{V}{kT}\int_0^\infty dt\langle P_{\alpha\beta}(0)P_{\alpha\beta}(t)\rangle . \quad (5)$$

where $\alpha\beta$ = xy, xz, yx, yz, zx, or zy and for a system of N molecules, the molecular formalism for the pressure tensor is given by

$$P_{\alpha\beta} = \frac{1}{V}\left[\sum_i m_i v_{i\alpha}v_{i\beta} + \sum_i \sum_{j>i} (r_{i\alpha} - r_{j\alpha})F_{ij\beta}\right]. \quad (6)$$

where the indices i and j refer to molecules i and j, and F_{ij} is the force between the centers of mass of molecules i and j. The Einstein relation is

$$\eta = \frac{1}{2kT}\frac{V}{t\to\infty}\lim \frac{d}{dt}\langle [Q_{\alpha\beta}(t) - Q_{\alpha\beta}(0)]^2\rangle . \quad (7)$$

where

$$Q_{\alpha\beta}(t) = \frac{1}{V}\sum_i m_i r_{i\alpha}(t)\cdot v_{i\beta}(t) . \quad (8)$$

Daivis and Evans showed that the tensorial property of the viscosity constant allows the use of all elements of the pressure tensor in the calculation of the viscosity to improve the statistics.[21] The system is isotropic in the absence of an external field so that the diagonal elements (the xx, yy, and zz components) are equal to give the scalar pressure $P=(P_{xx}+P_{yy}+P_{zz})/3$ and the off-diagonal elements (the xy, xz, and yz components) are also equal. The Green-Kubo relation, Eq. (5), becomes

$$\eta = \frac{V}{10kT}\int_0^\infty dt \sum_{\alpha\beta}\langle P_{\alpha\beta}(0)P_{\alpha\beta}(t)\rangle . \quad (9)$$

where $\alpha\beta$ = xx, yy, zz, xy, xz, yx, yz, zx, and zy,

$$P_{\alpha\beta} = (\sigma_{\alpha\beta} + \sigma_{\beta\alpha})/2 - \delta_{\alpha\beta}\left(\sum_\gamma \sigma_{\gamma\gamma}\right)/3 , \quad (10)$$

and

$$\sigma_{\alpha\beta} = \frac{1}{V}\left[\sum_i m_i v_{i\alpha}v_{i\beta} + \sum_i \sum_{j>i} (r_{i\alpha} - r_{j\alpha})F_{ij\beta}\right]. \quad (11)$$

The Einstein relation given by Eq. (7) cannot be used since $Q_{\alpha\beta}$ is not continuous under the periodic boundary condition.[22] Alternatively,

$$\eta = \frac{1}{20kT}\frac{V}{t\to\infty}\lim \frac{d}{dt}\langle \sum_{\alpha\beta}[Q_{\alpha\beta}(t) - Q_{\alpha\beta}(0)]^2\rangle . \quad (12)$$

where again $\alpha\beta$ = xx, yy, zz, xy, xz, yx, yz, zx, and zy.

Results and Discussion

Structural properties. Some equilibrium properties for liquid *n*-alkanes at several temperatures obtained from our MD simulations are listed in Table 2. To confirm the validity of our MD simulations, we compare the mean square radii of gyration (R_g^2), the two largest eigenvalues of the mass tesnor l_1^2 and l_2^2, and the mean square end-to-end distances (R_{ee}^2) of *n*-tetratetracontane (C_{44}) at 423 and 473 K with the previous MD simulation results[10] for united atom (UA) model. The values of R_g^2, l_1^2, l_2^2, and R_{ee}^2 of *n*-tetratetracontane from our MD results at 423 K and 0.742 g/cm^3 and at 473 K and 0.710 g/cm^3 (Table 2) are in good agreement with those from Ref. [10] [104(1), 0.804(4), 0.159(3), and 758(16) at 448 K and 0.766 g/cm^3, respectively]. Further comparison of self-diffusion constant and viscosity from Table 3 with the same

Table 2. Some structural properties of n-alkanes from our MD simulations

n-alkanes	T (K)	$\langle R_g^2(A^2)\rangle$	$\langle l_1^2/R_g^2\rangle$	$\langle l_2^2/R_g^2\rangle$	$\langle R_{ee}^2(A^2)\rangle$	$\langle R_{ee}^2\rangle/6\langle R_g^2\rangle$	*trans* (%)
n-$C_{12}H_{26}$	273	15.8(3)	0.919(1)	0.068(2)	139(5)	1.47(0)	75.4(1)
(-0.620)[a]	293	15.6(2)	0.914(1)	0.073(1)	136(2)	1.46(0)	73.7(2)
	311	15.4(1)	0.910(0)	0.076(0)	134(0)	1.45(0)	72.3(1)
	333	15.2(0)	0.907(0)	0.079(0)	131(0)	1.44(0)	70.8(1)
	372	14.9(0)	0.901(0)	0.084(0)	127(0)	1.42(0)	68.5(0)
n-$C_{20}H_{42}$	273	39.4(5)	0.903(4)	0.085(4)	354(7)	1.50(1)	77.3(5)
(-1.23)[a]	293	37.7(2)	0.891(2)	0.095(1)	330(2)	1.46(0)	74.7(1)
	311	36.8(1)	0.885(1)	0.100(1)	319(1)	1.44(0)	73.0(1)
	333	35.9(1)	0.879(1)	0.104(1)	308(1)	1.43(0)	71.5(1)
	372	34.7(1)	0.870(1)	0.111(1)	292(1)	1.40(0)	69.0(0)
n-$C_{32}H_{66}$	311	78.6(5)	0.853(2)	0.125(3)	652(9)	1.38(1)	73.7(2)
(-1.14)[a]	333	76.8(6)	0.848(3)	0.130(3)	617(8)	1.36(1)	71.9(1)
	372	71.3(2)	0.836(0)	0.138(0)	566(2)	1.32(0)	69.3(0)
	423	68.2(1)	0.830(2)	0.142(2)	533(5)	1.30(1)	66.7(0)
	473	65.6(2)	0.825(1)	0.145(1)	506(3)	1.29(0)	64.6(0)
n-$C_{44}H_{90}$	311	128(1)	0.833(6)	0.141(5)	1035(30)	1.32(1)	73.9(2)
(-1.43)[a]	333	124(1)	0.831(4)	0.141(3)	973(14)	1.30(1)	72.8(1)
	372	113(1)	0.817(3)	0.152(1)	860(13)	1.26(1)	69.5(1)
	423	107(1)	0.810(3)	0.156(2)	792(12)	1.24(1)	66.8(0)
	473	102(1)	0.805(3)	0.158(2)	750(10)	1.23(1)	64.7(0)

[a]The expansion coefficient in 10^{-3} K^{-1}.

Table 3. Some dynamic properties of n-alkanes from our MD simulations

n-alkanes	T (K)	D (Eq. 3)[a]	D (Eq. 4)	η (Eq. 9)[b]	η (Eq. 12)	Dη[c]	ζ_M[d]	τ_1 (ps)	τ_2 (ps)
n-$C_{12}H_{26}$	273	7.49(9)	7 51(10)	0.591(32)	0 593(22)	4.43	13.7(1)	175(3)	64.1(13)
	293	10 9(2)	10.8(1)	0.466(27)	0.467(28)	5.08	13.1(1)	112(3)	41.5(13)
	311	14.4(4)	14.4(5)	0.361(27)	0 365(29)	5.20	12.7(0)	83.1(5)	29 5(5)
	333	19.5(4)	19.4(4)	0.284(25)	0 280(29)	5.54	12.1(0)	58.6(8)	21 5(1)
	372	30.0(5)	29.9(6)	0.190(25)	0.188(24)	5.70	11.2(0)	35.6(4)	13 0(2)
n-$C_{20}H_{42}$	273	2 19(5)	2 21(5)	3.84(49)	3 79(26)	8.41	13.2(1)	1190(15)	422(13)
	293	3 53(7)	3.56(2)	2.51(29)	2.47(29)	8.86	12.8(1)	641(13)	232(4)
	311	5 07(7)	5 08(6)	1.79(23)	1 76(19)	9.08	12.4(0)	439(11)	161(4)
	333	7 36(12)	7.41(11)	1.26(25)	1 22(22)	9.27	11.9(0)	287(6)	107(2)
	372	12 3(1)	12.5(2)	0.767(17)	0.760(24)	9.43	11.1(0)	157(14)	59.7(14)
n-$C_{32}H_{66}$	311	2 01(6)	2 01(6)	9.54(34)	9 51(39)	19 2	12.2(1)	1440(41)	536(2)
	333	3 16(3)	3 20(5)	5.58(22)	5.55(34)	17 6	11.8(1)	942(16)	352(6)
	372	5.76(8)	5 79(8)	2.67(34)	2 71(36)	15.4	11.0(0)	469(11)	185(2)
	423	10 7(2)	10.8(2)	1.30(23)	1 26(20)	13.9	10.1(0)	265(9)	106(2)
	473	17 9(5)	17.3(3)	0.717(54)	0 708(32)	12.8	9.25(2)	164(2)	65.4(11)
n-$C_{44}H_{90}$	311	1 09(2)	1 10(2)	27.8(42)	27.3(45)	33 9	12.2(1)	2560(36)	969(47)
	333	1 80(3)	1.84(3)	15.0(48)	15.1(32)	29 5	11.7(1)	1620(30)	647(16)
	372	3.41(11)	3.42(9)	6.21(60)	6 23(62)	21.5	10.9(0)	840(23)	332(8)
	423	6.49(11)	6 52(8)	2.62(42)	2 57(32)	17.0	9.98(2)	465(16)	189(7)
	473	10 5(2)	10.5(2)	1.34(39)	1.40(37)	14.1	9.12(2)	302(8)	124(2)

[a]In 10^{-6} cm^2/sec. [b]In cP. [c]Obtained from D (Eq. 3) and η (Eq. 9). [d]In ps^{-1}.

previous MD simulation results[10] gives fairly reasonable agreement [5.27(30) and 2.30(5), respectively], considering the lower densities of our MD systems.

The change of R_g^2 over the whole temperature interval can be used to obtain an estimate of the expansion coefficient $k=d(\ln R_g^2)/dT$, which is given in Table 2. We also plot ($\ln R_g^2$) and ($\ln R_{ee}^2$) versus temperature in Figure 1. The obtained expansion coefficients of *n*-alkanes (C_{12}~C_{44}) are in the range of 0.62~1.43, which is in good agreement with the experimental value for bulk polyethylene $k = -1.07 \pm 0.08 \times 10^{-3}$ K^{-1}, obtained by SANS measurements.[23]

The largest eigenvalues (I_1^2) of the mass tensor corresponds to the smallest eigenvalue of the inertia tensor and the associated eigenvector defines the direction of the longest

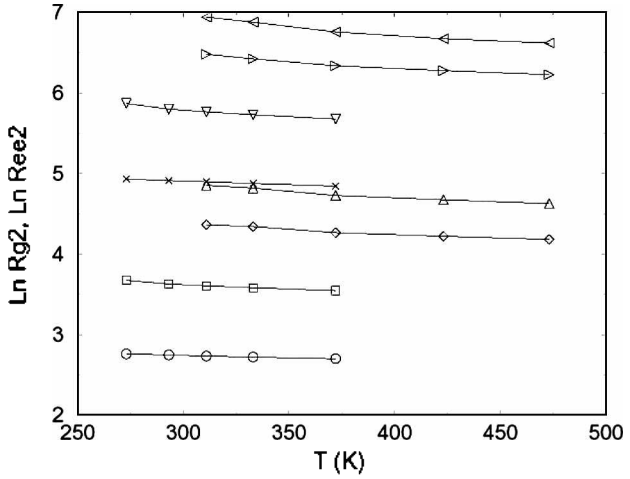

Figure 1. Plot of $\ln R_g^2$ (lower curves) and $\ln R_{ee}^2$ (upper curves) *vs.* T. From top, C_{44}, C_{32}, C_{20}, and C_{12}, respectively.

principal axis of the molecule's ellipsoid of inertia.[24] These eigenvalues (I_i^2) satisfy the relation $I_1^2 + I_2^2 + I_3^2 = R_g^2$ with $I_1^2 > I_2^2 > I_3^2$. As temperature increases, there is a decrease of I_1^2 and increases of I_2^2 and I_3^2, which reflects a reduction in the degree of asymmetry for *n*-alkanes (C_{12}~C_{44}). The largest eigenvalues (I_1^2) of the mass tensor also decreases with increasing chain length. For small chain length n, the chains are relatively rigid and the shape of the chain is of long ellipsoid. The physical picture here is that the chains of *n*-alkanes (C_{12}~C_{44}) are almost independent ellipsoids and the degree of asymmetry is reduced as temperature and chain length increase. Therefore, the chain dynamics is of the local segmental friction not the topological effect. The average fraction of C-C-C-C *trans* is found to decrease with increasing temperature, which coincides with the decrease of both R_g^2 and R_{ee}^2.

The crossover to the Rouse regime is examined by the ratio of the mean square end-to-end distances to the mean square radii of gyration as a function of the chain length, n. For Gaussian chains, it is satisfied that $\langle R_{ee}^2 \rangle = 6\langle R_g^2 \rangle = nb^2$ where b is the statistical segment length. The ratios of $\langle R_{ee}^2 \rangle / 6\langle R_g^2 \rangle$ for liquid *n*-alkanes at several temperatures obtained from our MD simulations are shown in Table 2. Clearly the ratio decreases with increasing temperature for all *n*-alkanes considered. At low temperatures for small $n \leq 20$, the ratio increases with increasing n since the chains are relatively rigid for small *n*. Figure 2 shows that at temperatures greater than 311 K, the ratio constantly decreases with increasing n and it is expected to approach the unity as n increases further. In the case of *n*-alkanes considered, the chains are clearly $\langle R_{ee}^2 \rangle / 6\langle R_g^2 \rangle >> 1$ and non-Gaussian. For *n*-alkanes, the crossover to Gaussian chain statistics is

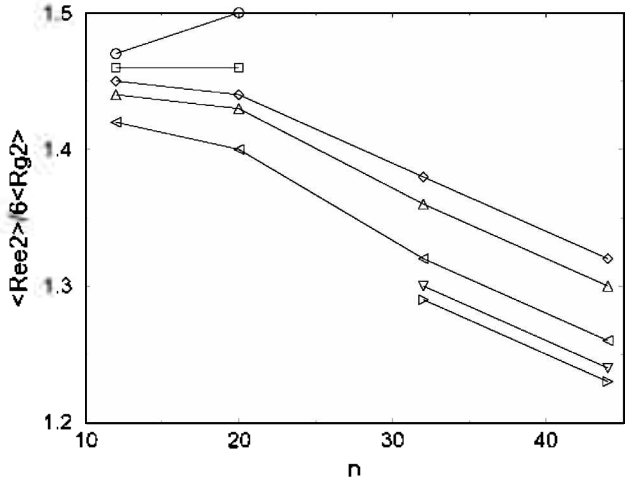

Figure 2. Plot of $\langle R_{ee}^2\rangle/6\langle R_g^2\rangle$ *vs.* chain length n. From top, T=273, 293, 311, 333, 372, 423, and 473 K, respectively.

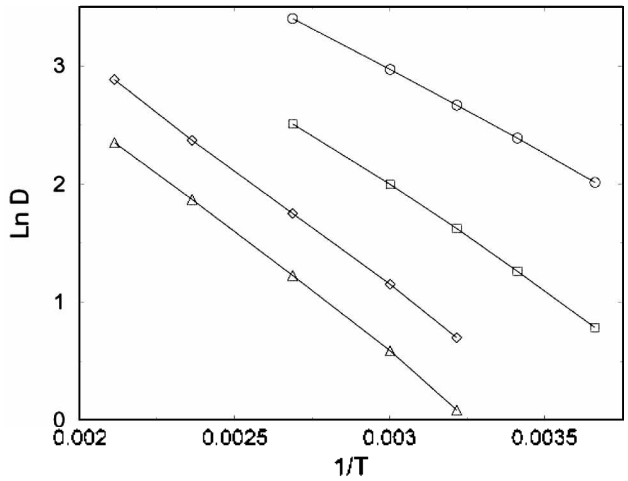

Figure 3. Arrhenius plot of D *vs.* 1/T. From top, C_{12}, C_{20}, C_{32}, and C_{44}, respectively.

known to occur for n greater than 100.[25-27] Since the Rouse model is based on the fact that the chains are Gaussian, one would expect that the crossover length is a minimum chain length for the Rouse model to hold, though this has not previously been checked systematically. Hence data from Table 2 for the ratio of $\langle R_{ee}^2\rangle/6\langle R_g^2\rangle$ implies that the liquid n-alkanes over the whole temperatures considered are far away from the Rouse regime.

Diffusion constant. Self-diffusion constants of n-alkanes D, obtained from both the Green-Kubo relation, Eq. (3), and the Einstein relation, Eq. (4), are collected in Table 3. The calculated diffusion constant of n-tetratetracontane (C_{44}) at 372 K are comparable with the previous MD simulation result[10] for a united atom (UA) model [4.52(21) at 400 K], though the results of both MD simulations overestimate the experimental measure [2.42(2) at 400 K].[28,29] The other previous MD simulation study[30] reported that the result of diffusion constants could be improved significantly by using an asymmetric united atom (AUA) model[31] which introduces a displacement between the centers of non-bonded interaction force and the centers of mass of the united atoms. In this study we do not consider the use of the AUA model since the qualitative trend of diffusion constants of liquid n-alkanes may not vary much on the model property.

The temperature dependence of the calculated diffusion constants of liquid n-alkanes over the whole temperatures considered are suitably described by an Arrhenius plot as shown in Figure 3:

$$D = D_0 \exp(-E_D/RT). \tag{13}$$

where D_0 is the pre-exponential factor. RT has the usual meaning, and E_D is the activation energy of n-alkane diffusion. The value of the activation energy is a direct measure of the temperature dependence of self-diffusion constant. The activation energies obtained from the slope of the least square fit are 2.83, 3.52, 3.91, and 4.06 kcal/mol for C_{12}, C_{20}, C_{32}, and C_{44}, respectively. The previous MD simulation study[30] reported this value as 3.98 kcal/mol for the UA model of n-tetracosane (C_{24}) which is compared with a value

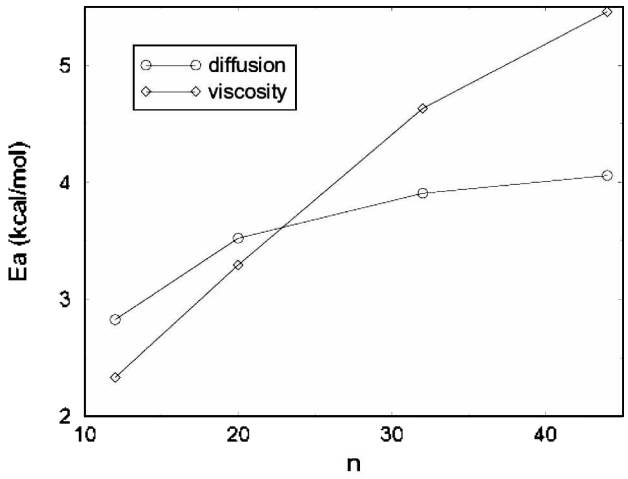

Figure 4. Activation energies of D (circle) and η (square) *vs.* chain length n.

of 4.04 kcal/mol obtained from viscosity measurements[32] and a value of 4.36 from PFG NMR results.[33] The values of E_D are plotted in Figure 4. As chain length n increases the increment of E_D decreases, and it is expected to approach an asymptotic value as n increases further. It was reported that E_D increases linearly with log M from 2.32 kcal/mol for n-heptane to 5.81 kcal/mol for n-hexacontane(C_{60}).[7,34] Fleisher[5] also determined E_D to be about 4.8 kcal/mol for several polyethylene independent of molecular weight from 9 to 52.7 kg/mol, from which we can deduce that E_D of n-alkane reaches an asymptotic limit over C_{60}.

We also show the log-log plot of diffusion constant versus molecular mass in Figure 5. The obtained exponents are between -2.43 and -1.58. Recent experimental study reported that $D \sim M^{-\alpha}$, with α changing approximately linearly from -2.72 to -1.85 as T increases.[7] Thus the apparent activation energy also rises linearly with log M. In the absence of molecular entanglements, Rouse kinetics predicts $\alpha = -1$, but Cohen-Turnbull-Bueche free-volume effects due to molecular chain ends add a further nonpower-law term,[35] enhancing D increasingly at low M.

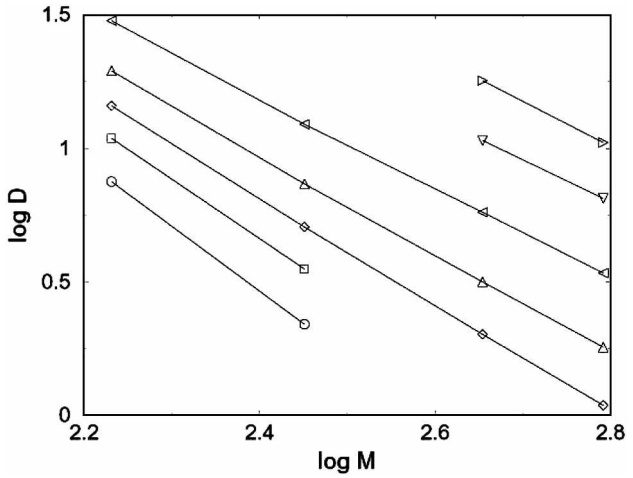

Figure 5. A log-log plot of D *vs.* M. From top, T = 473, 423, 372, 333, 311, 293, and 273 K, respectively.

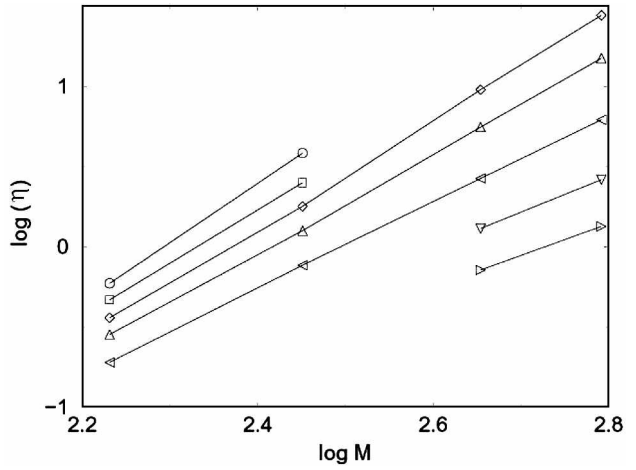

Figure 7. A log-log plot of η *vs.* M. From top, T = 273, 293, 311, 333, 372, 423, and 473 K, respectively.

Viscosity. Viscosities of *n*-alkanes η, obtained from both the Green-Kubo relation, Eq. (9), and the Einstein relation, Eq. (12), are collected in Table 3. The temperature dependence of the calculated viscosities of liquid *n*-alkanes over the temperatures are suitably described by an Arrhenius plot as shown in Figure 6:

$$\eta = \eta_0 \exp(E_\eta / RT) \tag{14}$$

where η_0 is the pre-exponential factor and E_η is the activation energy of *n*-alkane viscosity. But the experimental result for the linear polyethylene[6] showed that the lines are slightly curved, indicating that the temperature dependence, as in most polymers, does not follow the Arrhenius equation. The activation energies obtained from the slope of the least square fit are 2.33, 3.29, 4.63, and 5.46 kcal/mol for C_{12}, C_{20}, C_{32}, and C_{44}, respectively and are plotted in Figure 4. It was experimentally reported for *n*-alkanes and linear polyethylene[6] that the activation energy increases with chain length and at the highest molecular weight tested (M ~ 4.4 kg/mol) the activation energy reaches 6.6 kcal/mol, which is similar to the average value found for NBS 1482-4 (6.7 kcal/mol) and the values reported by others[36,37] for high molecular weight linear polyethylene (6.1-6.9 kcal/mol). The molecular weights of our *n*-alkanes considered in this study are in the range of 170-620 g/mol. However, as chain length *n* increases the increment of E_η decreases, and it is expected to approach an asymptotic value as M increases to the higher value.

Figure 7 shows the log-log plot of viscosity versus molecular mass. The obtained exponents are between 1.97-3.70. The experimental results for *n*-alkanes and linear polyethylene[6] show that h is well described by the power law $\eta \sim M^{1.8}$ at low molecular weight (M < 5 kg/mol) and $\eta \sim M^{3.64}$ at high molecular weight (M > 5 kg/mol) at 448 K. The molecular weight of the *n*-alkanes tested in this study is much lower than this experimental range of molecular weight, but the exponent for M = 450-620 g/mol gives 1.97 at 473 K.

In Figure 8, the logarithm of the product of ν and D versus log M is plotted, where ν is the kinematic viscosity, $\nu = \eta/\rho$. The slope decreases with increasing temperature and at 473 K νD becomes almost independent of M. It was reported

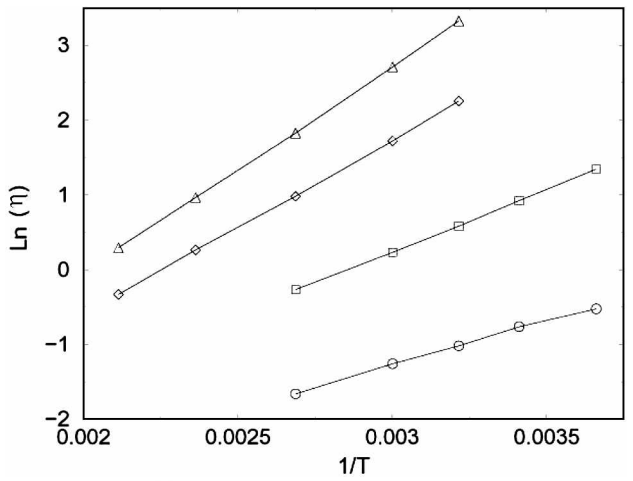

Figure 6. Arrhenius plot of η *vs.* 1/T. From top, C_{44}, C_{32}, C_{20}, and C_{12}, respectively.

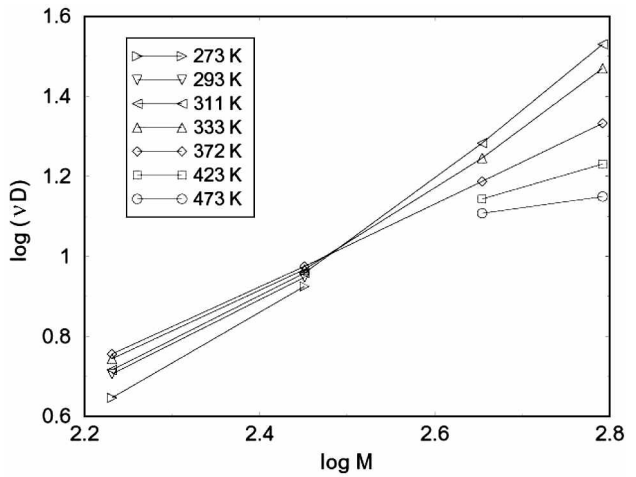

Figure 8. Log (νD) *vs.* log M.

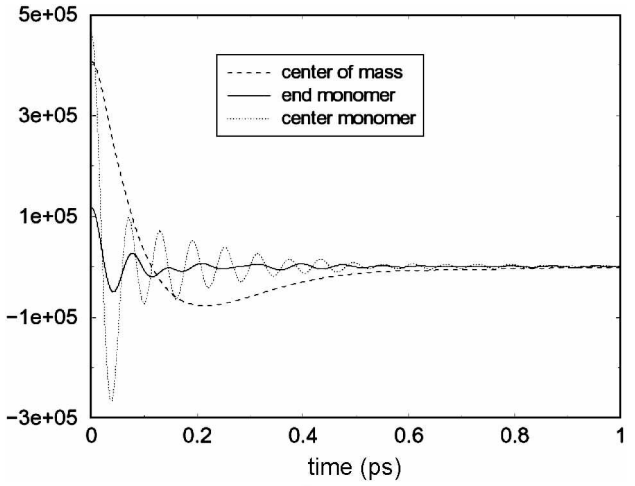

Figure 9. Force auto-correlation function of center of mass (dashed line), end monomer (solid line), and center monomer (dotted line) for *n*-tetratetracontane (C_{44}) at 473 K.

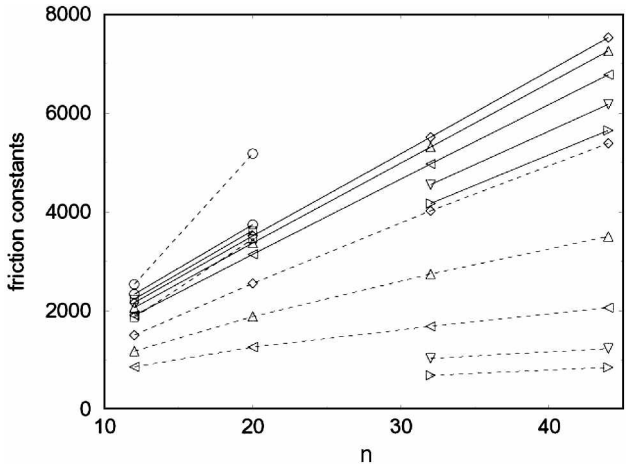

Figure 10. Friction constants (g/ps·mol), ζ (solid line) and ζ_D (dashed line), *vs.* chain length n. From top, T = 273, 293, 311, 333, 372, 423, and 473 K, respectively.

that for molecular weight M less than 5 kg/mol the product νD at 448 K is constant and then begins to increase like $M^{1.6}$ beyond M ~ 5 kg/mol. According to the Rouse and reptation models, this quantity should be equal to 1 in the unentangled regime (*i.e.*, for $M < M_e$) and equal to M/M_e for the entangled polymers (*i.e.*, for $M > M_e$). An M_e value of approximately 900 g/mol has been obtained for polyethylene.[38]

Friction constant. Molecular friction constant is obtained from the time integral of the force auto-correlation (FAC) function[39,40]:

$$\zeta_M = \frac{1}{\tau_r} = \frac{1}{MkT}\int_0^\tau dt \langle \mathbf{f}_i(0) \cdot \mathbf{f}_i(t) \rangle . \qquad (15)$$

where $\mathbf{f}_i(t) = \mathbf{F}_i(t) - \langle \mathbf{F}_i(t) \rangle$, $\mathbf{F}_i(t)$ is the total force exerted on molecule i, and τ_r is the macroscopic relaxation time of the FAC.[40] The force auto-correlation functions obtained from our MD simulations for liquid *n*-tetratetracontane (C_{44}) at 473.15 K only are shown in Figure 9. The FAC function for center of mass shows a well-behaved smoothly decaying curve, while those for center and end monomers are oscillating ones probably due to the rapidly varying interaction of methyl (or methylene) groups and it is impossible to calculate the monomeric friction constant directly from the FAC of each monomer. The initial decay of the FAC for center of mass is very rapid, occurring in a time ~0.2 ps, while a subsequent long tail decays only after several ps (not shown). It is well known that the calculation of friction constant from the force auto-correlation function is very hard due to the non-decaying long-time tails. As Kubo pointed out in his "fluctuation-dissipation theorem",[39] the correlation function of random force R will decay in a time interval of τ_c (microscopic time or collision duration time), whereas that of the total force F has two parts, the short time part or the fast similar to that of the random force and the slow part which should just cancel the fast part in the time integration.[41] This means that the time integral of Eq. (15) up to $t = \infty$ is equal to zero.

The time integral in Eq. (15) attains a plateau value for τ satisfying $\tau_c << \tau << \tau_r$, if the upper limit of the time integral, Eq. (15), is chosen that $\tau_c << \tau << \tau_r$ because the slow tail of the correlation function is cut off. However, we were unable to get the plateau value in the running time integral of the force auto-correlation function. Kubo suggested that the friction constants should be obtained from the random FAC function not from the total FAC and that there exists a difficulty to separate the random force part from the total force. We could obtain the friction constants by the time integral of the total FAC with choosing the upper limit of τ as the time that the FAC has the first negative value by assuming that the fast random force correlation ends at that time. Table 2 contains the molecular friction constants obtained from the time integral of the FAC using Eq. (15) and the estimated τ_r is in the range of 0.07-0.11 ps. The average monomeric friction constant (ζ) may be obtained by multiplying the molecular friction constant by molecular weight M or chain length n ($1/\zeta_M = M \times 1/\zeta$) and the other monomeric friction constant ζ_D is calculated from the self-diffusion constant D using Einstein relation, $\zeta_D = kT/nD$. Figure 10 shows ζ and ζ_D as a function of n. Both the friction constants, ζ and ζ_D, give a correct qualitative trend: decrease with increasing temperature and increase with increasing chain length n. An atomistic MD simulation of linear polyethylene melts[9] reported that the friction constant extracted from D by invoking the Rouse model is seen to increase from short alkanes to a chain-length-independent plateau, reached in a region of n=60-80. The linear increase of ζ and ζ_D with increasing n as shown in Figure 10 confirms again that the liquid *n*-alkanes over the whole temperatures considered are far away from the Rouse regime.

Global rotational motion. The global rotational motion of *n*-alkane molecules is characterized by the orientation relaxation of the end-to-end vector (**e**). Table 3 contains the results of the characteristic relaxation time τ calculated from the time auto-correlation function of the end-to-end vectors for four *n*-alkanes at several temperatures, where τ_1 and τ_2 indicate those of the first- and second-order orientation

correlation functions.

$$P_1^e(t) = \langle \mathbf{e}(t) \bullet \mathbf{e}(0) \rangle , \quad (16)$$

and

$$P_2^e(t) = \frac{1}{2}(3\langle [\mathbf{e}(t) \bullet \mathbf{e}(0)]^2 \rangle) - 1 , \quad (17)$$

In Figure 11 we show the first- and second-order orientaion correlation functions (Eqs. (16) and (17)) of the end-to-end vector for *n*-dodecane (C_{12}) and *n*-tetratetracontane (C_{44}) at 311 and 333 K. A simple exponential can always adequately describe the relaxation behavior of the end-to-end vectors. The characteristic relaxation time decreases with increasing temperature and it increases with increasing chain length n. In the case of isotropic rotational diffusion a value of 3 for the ratio τ_1/τ_2 is expected.[42,43] The ratios τ_1/τ_2 obtained from the characteristic times are in the range between 2.70-2.82 for *n*-dodecane (C_{12}), 2.63-2.82 for *n*-eicosane (C_{20}), 2.50-2.69 for *n*-dotriacontane (C_{32}), and 2.50-2.64 for *n*-tetratetracontane (C_{44}) which are closed to 3. This ratio appears to decrease with increasing chain length n, which is contrasted with the reduction in the degree of asymmetry for *n*-alkanes (C_{12}-C_{44}) with chain length n. It is hard to reach a detailed conclusion on the temperature and chain length dependence with given statistical uncertainty.

The Rouse model also predicts a relation for the relaxation of the time autocorrelation function of the end-to-end vector **e** as [44]

$$\frac{\langle \mathbf{e}(t) \bullet \mathbf{e}(0) \rangle}{\langle e^2 \rangle} = \sum_{p=1,3,} \frac{8}{p^2\pi^2} \exp\left(-\frac{tp^2}{\tau_{ee}}\right), \quad (18)$$

where τ_{ee} is the longest relaxation time expressed as

$$\tau_{ee} = \frac{\zeta_o n^2 \langle R_{ee} \rangle^2}{3\pi^2 kT} \quad (19)$$

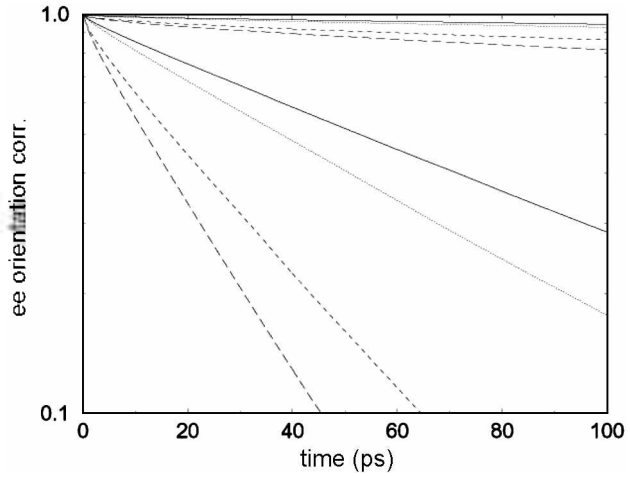

Figure 11. First-order (P_1^e, Eq. (16)) and second-order orientation correlation functions (P_2^e, Eq. (17)) of the end-to-end vector for *n*-tetratetracontane (C_{44}) (upper curves) and for *n*-dodecane (C_{12}) (lower curves). The solid, dotted, dashed, and long dashed lines are for P_1^e at 311 and 333 K, and P_2^e at 311 and 333 K, respectively.

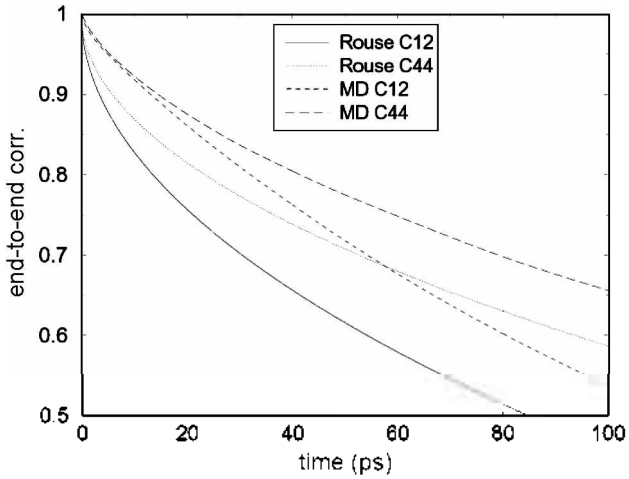

Figure 12. Comparison of time auto-correlation functions of the end-to-end vector calculated from Eq. (18) using τ_{ee} = 170 ps for *n*-dodecane (C_{12}) at 273 K and using τ_{ee} = 302 ps for *n*-tetratetracontane (C_{44}) at 473 K with those extracted directly from our MD simulations.

where ζ_o is the monomeric friction constant. From Eq. (18), it is obvious that the autocorrelation function of the end-to-end vector is clearly dominated by the first (p = 1) mode. In Figure 12 we compared the time auto-correlation function of the end-to-end vector as calculated from Eq. (18) using τ_{ee} = 170 ps for *n*-dodecane (C_{12}) at 273 K and using τ_{ee} = 302 ps for *n*-tetratetracontane (C_{44}) at 473 K, and as extracted directly from our MD simulations. The figure shows again that the short chain *n*-alkane is far away from the Rouse regime.

Conclusion

In this paper we have presented the results for viscosity and self-diffusion constants of model systems for four liquid *n*-alkanes in a canonical (NVT) ensemble at several temperatures using molecular dynamics simulations. The small chains of these *n*-alkanes are clearly $\langle R_{ee}^2 \rangle / 6 \langle R_g^2 \rangle \gg 1$. This result leads to the conclusion that the liquid *n*-alkanes over the whole temperatures considered are far away from the Rouse regime, though the ratio becomes close to the unity as chain length increases. Calculated self-diffusion constants D are comparable with experimental results and the temperature dependence of the calculated diffusion constants is suitably described by the Arrhenius plot. The calculated activation energies are in good agreement with other MD simulation study and NMR results. The temperature dependence of the calculated viscosity η is also well described by the Arrhenius plot, which is contrasted with the experimental result for the linear polyethylene showing that the lines are slightly curved. The behavior of the activation energy E_η with increasing chain length indicates that the activation energy approaches an asymptotic value as n increases to the higher value, which is experimentally observed. The average monomeric friction constant ζ calculated directly from the FAC function and the other

monomeric friction constant ζ_D calculated from the Einstein relation give a correct qualitative trend: decrease with increasing temperature and increase with increasing chain length n. The linear increase of ζ and ζ_D with increasing n confirms that the liquid *n*-alkanes over the whole temperatures considered are far away from the Rouse regime. Comparison of the time auto-correlation functions of the end-to-end vector calculated from Eq. (18) using τ_{ee} = 170 ps for *n*-dodecane (C_{12}) at 273 K and using τ_{ee} = 302 ps for *n*-tetratetracontane (C_{44}) at 473 K with those extracted directly from our MD simulations also supports that the short chain *n*-alkanes considered in this study are far away from the Rouse regime. The characteristic relaxation time of the orientation correlation of the end-to-end vector decreases with increasing temperature and it increases with increasing chain length n. In the case of isotropic rotational diffusion a value of 3 for the ratio τ_1/τ_2 is expected, but the ratios τ_1/τ_2 obtained from our MD simulations are in the range between 2.50-2.82 for *n*-alkanes considered in this study. To approach the Rouse regime, it is necessary to extend MD simulation for longer *n*-alkanes such as C_{88} and C_{132}, and those systems are presently under study.

Acknowledgment. This research was supported by a Korea Research Foundation Grant (KRF-2000-015-DP0185).

References

1. Berry, G. C.; Fox, T. G. *Adv. Polym. Sci.* **1968**, *5*, 261.
2. Tirrell, M. *Rubber Chem. Technol.* **1984**, *57*, 523.
3. Lodge, T. P.; Rotstein, N. A.; Prager, S. *Adv. Chem. Phys.* **1990**, *9*, 1.
4. Ferry, J. D. *Viscoelastic Properties of Polymers*, 3rd ed.; Wiley: New York, 1980.
5. Fleisher, G. *Polym. Bull.* (Berlin) **1983**, *9*, 152.
6. Pearson, D. S.; Ver Strate, G.; von Meerwall, E.; Schilling, F. C. *Macromolecules* **1987**, *20*, 1133.
7. Von Meerwall, E.; Beckman, S.; Jang, J.; Mattice, W. L. *J. Chem. Phys.* **1998**, *108*, 4299.
8. De Gennes, P.-G. *Scaling Concepts in Polymer Physics*; Cornell University Press: Ithaca, New York, 1979.
9. Harmandaris, V. A.; Mavrantzas, V. G.; Theodorou, D. N. *Macromolecules* **1998**, *31*, 7934.
10. Mondello, M.; Grest, G. S.; Webb, E. B.; Peczak, P. *J. Chem. Phys.* **1998**, *109*, 798.
11. Park, H. S.; Chang, T.; Lee, S. H. *J. Chem. Phys.* **2000**, *113*, 5502.
12. Mundy, C. J.; Siepmann, J. I.; Klein, M. L. *J. Chem. Phys.* **1995**, *102*, 3376.
13. Cui, S. T.; Cummings, P. T.; Cochran, H. D. *J. Chem. Phys.* **1996**, *104*, 255.
14. Cui, S. T.; Gupta, S. A.; Cummings, P. T.; Cochran, H. D. *J. Chem. Phys.* **1996**, *105*, 1214.
15. Evans, D. J. *J. Chem. Phys.* **1983**, *78*, 3297.
16. Brown, D.; Clarke, J. H. R. *Mol. Phys.* **1984**, *51*, 1243.
17. Andersen, H. J. *Comput. Phys.* **1984**, *52*, 24.
18. Jorgensen, W. L.; Madura, J. D.; Swenson, C. J. *J. Am. Chem. Soc.* **1984**, *106*, 6638.
19. Allen, M. P.; Tildesley, D. J. *Computer Simulation of Liquids*; Oxford Univ. Press: Oxford, 1987; p 81.
20. McQuarrie, D. A. *Statistical Mechanics*; Harper and Row: New York, 1976.
21. Daivis, P. J.; Evans, D. J. *J. Chem. Phys.* **1994**, *100*, 541.
22. Haile, J. M. *Molecular Dynamics Simulation*; Wiley: New York, 1992.
23. Boothroyd, A.; Rennie, A. R.; Boothroyd, C. B. *Europhys. Lett.* **1991**, *15*, 715.
24. Goldstein, H. *Classical Mechanics*; Addison-Wesley: Harvard University, 1974.
25. Baschnagel, J.; Qin, K.; Paul, W.; Binder, K. *Macromolecules* **1992**, *25*, 3117.
26. Brown, D.; Clarke, J. H. R.; Okuda, M.; Yamazaki, T. *J. Chem. Phys.* **1994**, *100*, 1684; *ibid* **1996**, *104*, 2078.
27. Paul, W.; Smith, G. D.; Yoon, D. Y. *Macromolecules* **1997**, *30*, 7772.
28. Paul, W.; Yoon, D. Y.; Smith, G. D. *J. Chem. Phys.* **1995**, *103*, 1702.
29. API 42. *Properties of Hydrocarbons of High Molecular Weight*; American Petroleum Institute: Research Project 42, Washington, D. C., 1966.
30. Mondello, M.; Grest, G. S. *J. Chem. Phys.* **1995**, *103*, 7156.
31. Padilla, P.; Toxvaerd, S. *J. Chem. Phys.* **1991**, *94*, 5650; *ibid.* **1991**, *95*, 509.
32. Nederbragt, G. W.; Boelhouwer, J. W. M. *Physica* **1947**, *13*, 305.
33. See page 7161 in Reference 30.
34. Ertl, H.; Dullien, F. A. L. *AIChE J.* **1973**, *19*, 1215.
35. Cohen, M. H.; Turnbull, D. *J. Chem. Phys.* **1959**, *31*, 1164.
36. Mendelson, R. A.; Bowles, W. A.; Finer, F. L. *J. Polym. Sci.*, Part A-2, **1970**, *8*, 105.
37. Raju, V. R.; Smith, G. G.; Marin, G.; Knox, J. R.; Graessley, W. W. *J. Polym. Sci., Polym. Phys. Ed.* **1979**, *17*, 1183.
38. Carella, J. M.; Graessley, W. W.; Fetters, L. J. *Macromolecules* **1984**, *17*, 2775.
39. Ciccotti, G.; Ferrario, M.; Hynes, J. T.; Kapral, R. *J. Chem. Phys.* **1990**, *93*, 7137.
40. Kubo, R. *Rep. Prog. Phys.* **1966**, *29*, 255.
41. Kubo approximately described these two force auto-correlation functions in his original papers, see Figure 2 in Ref. 40.
42. Debye, P. *Polar Molecules*; Dover: New York, 1929.
43. Berne, B.; Pecora, R. *Dynamic Light Scattering*; Wiley: New York, 1976.
44. Doi, M.; Edwards, S. F. *The theory of Polymer Dynamics*; Clarendon: Oxford, 1986.